

## CXRS measurements of energetic helium ions in ASDEX Upgrade plasmas heated with a three-ion species ICRH scheme

A. Kappatou<sup>1</sup>, M. Weiland<sup>1</sup>, R. Bilato<sup>1</sup>, Ye. O. Kazakov<sup>2</sup>, R. Dux<sup>1</sup>, V. Bobkov<sup>1</sup>, B. Geiger<sup>1</sup>, T. Pütterich<sup>1</sup>, R.M. McDermott<sup>1</sup>, the EUROfusion MST1\* and the ASDEX Upgrade teams

<sup>1</sup>*Max-Planck-Institut für Plasmaphysik, Garching, Germany*

<sup>2</sup>*Laboratory for Plasma Physics, LPP-ERM/KMS, Brussels, Belgium*

\* *See the author list of H. Meyer et al., Nucl. Fusion 57, 102014 (2017)*

### Introduction

The generation and investigation of energetic helium in present devices can provide insight on how fusion-produced, fast alpha particles will behave in future reactor plasmas. Aside from investigating fusion-produced He (TFTR [1]), a fast He population can be simulated either by He neutral beam injection (NBI) (JET [2]), or by using ion cyclotron resonance heating (ICRH) to accelerate either <sup>4</sup>He-beam ions (JET [3]) or <sup>3</sup>He ions (TFTR [4]). A key element in such studies is the measurement of the fast He populations with charge exchange recombination spectroscopy (CXRS) [1, 2, 4]. CXRS measurements of energetic <sup>3</sup>He ions, a new measurement for ASDEX Upgrade (AUG), are presented.

### Charge exchange spectroscopy for measurements of thermal and energetic helium

CXRS provides the impurity ion temperature, rotation and density, from the Doppler broadening, the Doppler shift and the intensity of the measured CX emission line, respectively. The most commonly used spectral line for He measurements is at 468.571 nm (n=4-3 transition). The interpretation of the He CX spectra is not straightforward, as it is comprised of many components: the active charge exchange emission, the passive emission and the He “plume” emission. An energetic He population with energies higher than the thermal population contributes an additional emission, in the wings of the He spectral line, at higher and/or lower wavelengths. The intensity of the energetic He signal depends on the amount of energetic ions in the plasma and on their relative velocity with respect to the neutral beam used for CXRS.

### Plasma scenario

An energetic helium signal was observed in the CX spectra in experiments investigating the feasibility of a novel “three-ion species” ICRH scheme at AUG [5, 6]. A mixed H-D plasma ( $n_H/n_e \sim 70\%$ ) was heated successfully with a small amount of energetic <sup>3</sup>He ions generated with ICRH, as resonant minority species with  $Z/A$  between that of the two main ions. An important difficulty associated with the application of this scheme on AUG is controlling the desired low <sup>3</sup>He concentrations ( $c_{^3He}$ ) at  $\sim 0.5 - 2\%$ , in the absence of a real-time control scheme.

The plasma discharge #34704 is used herein as an example ( $B_t = -2.8$  T,  $I_p = 0.8$  MA). Core  $c_{^3He}$  of 0.5-1% were achieved by short puffs (50 ms long, every 0.5 s,  $2.3 \cdot 10^{20}$  e/s). Hydrogen neutral beams were used ( $P_{NBI} \sim 8$  MW, 53 keV). The ICRH power was increased in steps 0, 0.9, 1.9 and 2.5 MW ( $f = 30$  MHz, dipole phasing), with the resonance deliberately

located at  $\rho_{\text{pol}} \sim 0.3$  on the high-field side to reduce the fast ion energies and thus improve the confinement of the RF-heated  $^3\text{He}$  ions. High-field side off-axis  $^3\text{He}$  heating with the three-ion species scenario was recently suggested as a potential option for H-mode studies in ITER [7].

### Spectral signature of energetic helium in the three-ion ICRF scheme heated plasmas

Examples of the measured He spectra in #34704 are shown in Fig. 1(a) for one diagnostic line-of-sight (LOS), corresponding to  $\rho_{\text{pol}} \sim 0.3$ . The time points correspond to the different levels of  $P_{\text{ICRH}}$ . The passive, “plume” and thermal active emissions are around the nominal HeII wavelength (468.571 nm). The emission corresponding to the energetic  $^3\text{He}$  population can be seen at wavelengths  $> 470$  nm and  $< 468$  nm.  $^3\text{He}$  and  $^4\text{He}$  cannot be distinguished in the CXRS measurements. Since the ICRH scheme applied here, however, accelerates efficiently mainly the  $^3\text{He}$  ions, any signal corresponding to non-thermal populations can be attributed to  $^3\text{He}$ . A number of smaller emission lines, most probably associated with W ( $c_w = 0.6 - 1.2 \cdot 10^{-4}$ ), disturb the spectra.

Without ICRH, no energetic population is observed (red spectrum). With increasing  $P_{\text{ICRH}}$ , the intensity of this emission increases (blue, green and purple spectra), without significant changes in the plasma parameters. In Fig. 1(b), the CX intensity is plotted as a function of the energy of the ions along the LOS (velocity component along the LOS) for the different time points (and  $P_{\text{ICRH}}$  levels). The shaded wavelength ranges indicated in the spectra are used to avoid any disturbing emission lines and the patterned range is used for the background subtraction. The energetic signal corresponds to ions with energy larger than  $\sim 10$  keV projected on the LOS. In Fig. 1(c), the CX intensity at  $t = 3.6$  s is shown for different plasma locations. The signal is higher at  $\rho_{\text{pol}} \sim 0.3$  and lower towards the magnetic axis and the plasma mid-radius. Further outside, no energetic signal is observed.

The observation geometry is important in understanding the value of energy along LOS. The CXRS system has a toroidal view on the AUG NBI box I and is focused on source #3, but intersects all NBI box I sources (in this pulse, sources #2-#4 were on).

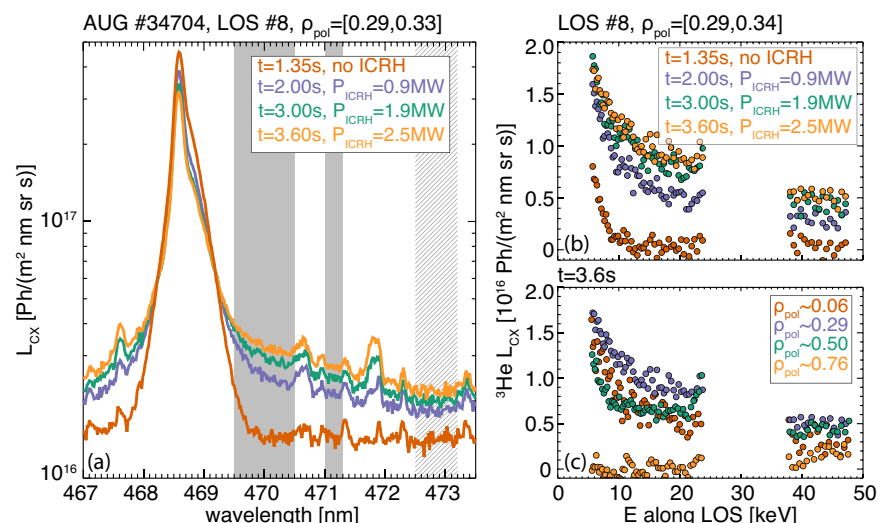


Fig. 1: (a) Measured CX spectra for one LOS at different times and  $P_{\text{ICRH}}$  levels during #34704, (b) CX intensity as a function of the ion energy projected on to the LOS for the wavelength ranges identified on the spectra at the these time points at  $\rho_{\text{pol}} \sim 0.3$  and (c) across  $\rho_{\text{pol}}$  at  $t = 3.6$  s. The patterned wavelength range is used for the background subtraction.

## Comparison with TORIC-SSFPQL

While obtaining the distribution function of the  ${}^3\text{He}$  ions from the CXRS measurement is not straightforward, the expected spectral radiance  $L_\lambda$  can be evaluated from the distribution function  $f_{{}^3\text{He}}$  obtained from modelling as follows:

$$L_\lambda = \frac{1}{4\pi} \sum_{E=1}^4 \sum_{m=1}^2 \int_{v=0}^{v_{\max}} \int_{p=-1}^1 \int_{\phi=0}^{2\pi} v^2 f_{{}^3\text{He}}(v, p) \langle \sigma_{\text{CX}}(v_{\text{col}}) v_{\text{col}} \rangle_{E,m} \int_{\text{LOS}} n_b^{E,m}(l) \text{d}l \times \delta \left[ \lambda - \lambda_0 \left( 1 + \frac{v}{c} \cos \theta \right) \right] \text{d}\phi \text{d}p \text{d}v. \quad (1)$$

Here,  $\lambda$  corresponds to the wavelength, with  $\lambda_0 = 468.571$  nm and the integration is performed over velocity  $v$  and over the pitch angles  $p = \cos(v_{\parallel}/v)$ . The density of the beam neutrals  $n_b^{E,m}$ , where  $E$  corresponds to the three beam energy components and the beam halo and  $m$  to the main quantum number of the neutrals, is calculated with a collisional-radiative model [8]. The effective charge exchange emission cross sections  $\sigma$  depend on the collision velocity  $v_{\text{col}}$  between the ion and the beam neutral.  $\theta$  is the angle between the LOS and the ion velocity. The fast ion velocity has a pitch angle to the magnetic field line and an angle  $\phi$  to the other perpendicular direction to the field line. The distribution function at the effective measurement location of the LOS is considered, and it is assumed that the distribution function, the local plasma parameters and consequently the CX emission rates do not vary strongly along the LOS and only  $n_b^{E,m}$  is integrated along the CXRS LOS with coordinate  $l$ .

The distribution function at 3.6 s ( $\text{PICRH} = 2.5$  MW), shown in Fig. 2(a) for  $\rho_{\text{pol}} = 0.3$ , was obtained with TORIC-SSFPQL, a coupling of the full-wave solver TORIC and the Fokker-Planck quasilinear solver SSFPQL [9] assuming  $c_{{}^3\text{He}} = 0.6\%$ . This value is derived ignoring the tails of the CX spectrum and corresponds to the total He content. Here, it is assumed that all He in the plasma is  ${}^3\text{He}$ , however, some  ${}^4\text{He}$  is still present. Since it is not straightforward to model the He spectra in their entirety, due to the number of different contributions and the additional W lines, this is only an estimate to provide a starting point. Furthermore, the full spectrum of the antenna was modelled, but no orbit losses and broadening or redistribution of the profiles are considered.

The parallel and perpendicular temperature of the TORIC-SSFPQL distribution function,  $T_{\parallel}$  and  $T_{\perp}$ , respectively, can be seen in Fig. 2(b). The CXRS LOS are toroidal with angles  $< 20^\circ$  to the magnetic field and sample predominantly  $T_{\parallel}$  which reaches up to 15 keV (but also  $T_{\perp} \sim 0.5$  MeV). An energetic signal is expected only in the region  $0.15 < \rho_{\text{pol}} < 0.55$ . The predicted CX intensity from Eq. 1, as a function of the energy projected on the LOS is shown in Fig. 2(c) (circles). Comparing with Fig. 1(c), one sees that in the energy range 15-20 keV, the predicted intensities are  $< 40\%$  lower than the ones measured by CX at  $\rho_{\text{pol}} = 0.29$  and  $< 20\%$  lower at  $\rho_{\text{pol}} = 0.50$ . Both the measurement and the prediction show no energetic signal further outside than mid-radius. In contrast to the CX measurement, no energetic He signal is expected close to the plasma core. Since the ICRH resonance was on the high field side, many trapped

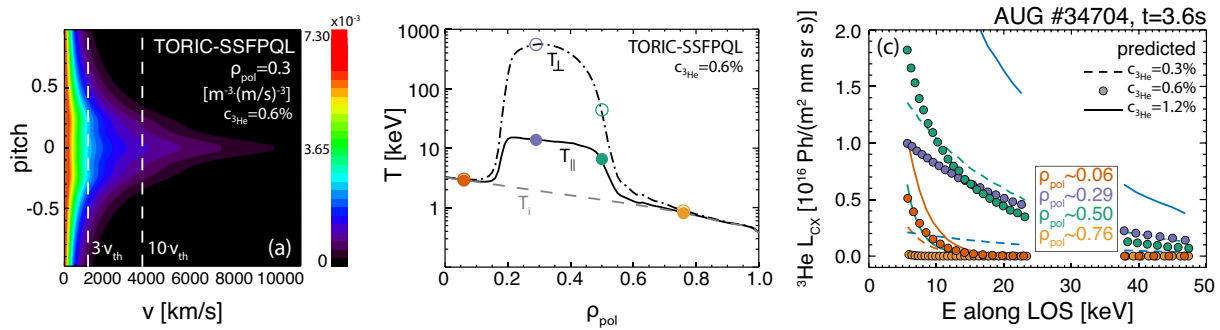


Fig. 2: (a) Distribution function obtained with TORIC-SSFPQL for #34704 at 3.6 s and  $\rho_{pol} = 0.3$ , assuming  $c_{^3He} = 0.6\%$ , (b) parallel temperature of the distribution function, with the LOS measurement locations shown in Fig. 1(c), (c) predicted CX intensity as a function of the ion energy along the LOS across  $\rho_{pol}$ . The same wavelength ranges as in Fig. 1 are used.

energetic particles resonating with the ICRH waves might have orbits with banana widths large enough to explore also the region close to the magnetic axis. SSFPQL is based on the zero-banana-width approximation, and as such this effect would not be captured in this simulation.

As the efficiency of the heating scheme and the TORIC-SSFPQL result depend critically on the exact  $^{^3}\text{He}$  concentration, which is difficult to pinpoint in this situation, its influence on the predicted spectra was assessed. The effect of using a lower ( $c_{^3}\text{He} = 0.3\%$ , dashed lines) and higher concentration ( $c_{^3}\text{He} = 1.2\%$ , solid lines) is shown in Fig. 2(c)). In the energy range 15-20 keV a  $^{^3}\text{He}$  concentration slightly higher than 0.6% can bring the prediction within a difference 30% of the measurement at both  $\rho_{pol} = 0.29$  and  $\rho_{pol} = 0.50$ .

## Discussion and conclusions

CXRS measurements of energetic  $^{^3}\text{He}$  ions at AUG are presented for a special three-ion species ICRH scheme which preferentially accelerated  $^{^3}\text{He}$  ions. The measured CX spectra are compared with modelled spectra evaluated using TORIC-SSFPQL distribution functions. The magnitude of the predicted CX spectral radiance and the expected energies of the ions that undergo CX agree very well with the measurement, confirming that the wings in the CX spectra are due to ICRF-accelerated  $^{^3}\text{He}$ . However, differences are observed that can be attributed to physics not included in the modelling and more advanced modelling is required in the future. CXRS can provide important information on the confined energetic He ions, which can be used for validation of fast ion and ICRH modelling codes for use in current and future devices.

This work has been carried out within the framework of the EUROfusion Consortium and has received funding from the Euratom research and training programme 2014-2018 under grant agreement No 633053. The views and opinions expressed herein do not necessarily reflect those of the European Commission.

## References

- [1] G.R. McKee *et al*, Nucl. Fusion **37**, 501 (1997)
- [2] M.G. von Hellermann *et al*, Plasma Phys. Control. Fusion **35**, 799 (1993)
- [3] M.J. Mantsinen *et al*, Phys. Rev. Lett. **88**, 105002 (2002)
- [4] B.C. Stratton *et al*, Nucl. Fusion **34**, 734 (1994)
- [5] Ye.O. Kazakov *et al*, Nat. Phys. **13**, 973 (2017)
- [6] Ye.O. Kazakov *et al*, contribution submitted to the 27th IAEA Fusion Energy Conference (2018)
- [7] M. Schneider *et al*, EPJ Web Conf. **157**, 03046 (2017)
- [8] R. McDermott *et al*, Plasma Phys. Control Fusion, *submitted*
- [9] R. Bilato *et al*, Nucl. Fusion **51**, 103034 (2011)